LAD Error Optimization

Sara Ratliff[1], Tyler Kutz[1], and Axel Schmidt[1]

[1]George Washington University

June 18, 2021

1 Introductory Material

In the original LAD proposal [1], the spectrometer settings were chosen based on a simulation that considered experimental conditions expected in 2011, at the time of the proposal. Between then and now, a number of specific details about the LAD experiment have changed: we plan to use a pair of GEM detectors for vertexing, the luminosity will be larger, and the placement of the LAD panels has been adjusted around space constraints in Hall C. In this work, we use the fast Monte Carlo simulation developed in the "`deuteron_dis`" repository to re-optimize the spectrometer settings with these new conditions and test the feasibility of increasing the high-x' threshold.

The simulation software used can be found on github under

- `https://github.com/schmidta87/deuteron_dis`
- commit ID: `89684cbbf1fb44d6b519c16d8a13ae849b30d7c9`

The programs `dis_HallC`, `inclusive_HallC`, and `randoms_HallC` were used for initial event generation. The generated events were then passed through a series of programs: `lad_sim` to simulate trajectories, `lad_digi` to model detector response and reconstruct events, and `lad_analysis` to perform event selection. Once run through these programs, we conducted an analysis of the ideal settings to minimize statistical error, by optimizing with respect to the time distribution in each setting (high and low x' settings), the high and low x' angular positions, and the common momentum setting.

The results of this analysis find that if one adopts the same high-x' threshold used in the original LAD proposal ($x' > 0.45$), the settings are already very well optimized. However, if we wish to adopt a threshold of $x' > 0.5$, we would benefit from spending a significantly larger proportion of time in the high x' angular position.

2 Generator

The simulation starts with an event generator. We have developed two event generators, one for signal events, one for background, and these are described in the sections below. Both are based on the same theory calculations used for making rate estimates in the LAD proposal.

2.1 Tagged-DIS Generator

The signal generator models the process of tagged deep inelastic scattering (Tagged-DIS) from a neutron in deuterium, in which an electron scatters in high Q^2 and high W kinematics in coincidence with a spectator proton recoiling from the deuteron. Our generator is based on a PWIA cross section model developed by Wim Cosyn and Misak Sargsian [2]. It is identical to the cross section model used for rate estimates in the proposal.

We built an event generator using ROOT's `TFoam` class, using adaptive sampling to produce an unweighted event sample. The generator is based on a similar generator that was written for preliminary

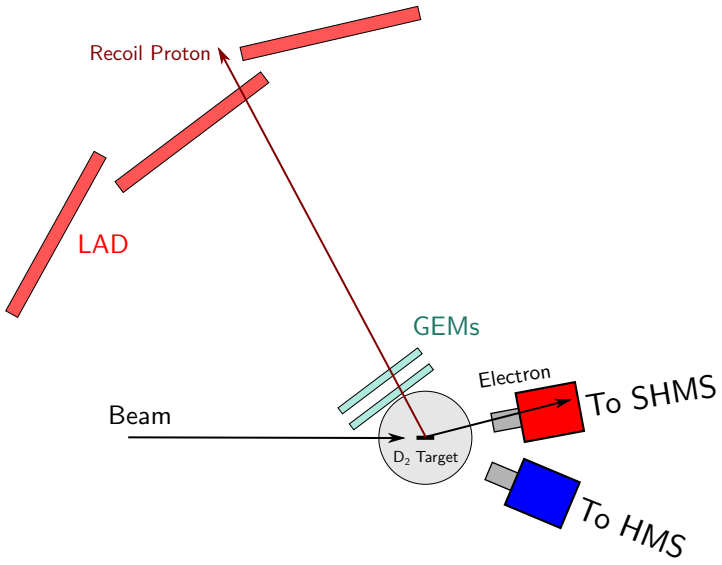

Figure 1: An overhead view of the LAD Experiment

BAND simulations (e.g., those referenced in the BAND ERR presentations [3]). In addition to producing kinematics for each event, the `TFoam` class also calculates the total cross section within the chosen generation range. We chose to generate over different ranges for detection in the HMS and SHMS, detailed in table 1. Using 10.9 GeV for the beam energy, the total cross section over the generation range is 50.3 pb in HMS mode, and 34.3 pb in SHMS mode. These generation ranges are meant to cover all of the possible phase space that the spectrometers could feasibly reach, not to represent the specific spectrometer acceptances in a single setting.

Table 1: Generation ranges for the two spectrometers

Spectrometer	θ-range [°]	ϕ-range [°]	Mom. range [GeV/c]
HMS (e^-)	8–24	180 ± 25	0.4–9.0
SHMS (e^-)	8–24	± 25	1.8–10.0
LAD (p)	87–160	± 50	0.2–1.0

2.2 Random Coincidence Background

The principle background in LAD is random coincidence background, in which an electron is detected in a spectrometer in coincidence with an unrelated proton detection in LAD. The rate of random coincidence background, R_{randoms}, scales as:

$$R_{\text{randoms}} \propto \sigma_{e^-} \sigma_p \mathcal{L}^2 \Delta t, \tag{1}$$

where σ_{e^-} is the cross section for detecting a single electron, σ_p is the cross section for detecting a single proton, $\mathcal{L}$ is the instantaneous luminosity, and Δt is the coincidence time window. A random coincidence background generator therefore needs to model both the single electron cross section, the single proton cross section, and randomly offset them in time by some interval Δt.

Single electrons were modeled using the inclusive cross section model of Cosyn and Sargsian [2]. This is the same model as used in the LAD Proposal. An identical generation range was chosen and the total generated cross section was found to be 13.0 nb for the HMS mode, and 15.9 nb for the SHMS mode.

The model for the single protons rates was based on that used in the proposal. The proposal assumed that LAD would see an isotropic rate of 1 MHz/sr for protons with a momentum above 250 MeV/c, assuming a luminosity of 2×10^{36} cm^{-2}s^{-1} per nucleon (i.e., 10^{36} cm^{-2}s^{-1} per deuteron). The simulation described

in this work required some information about the momentum spectrum of the singles protons, and this was inferred by fitting data in Table 8 of the proposal [1]. The results of the fit are shown in Fig. 2.

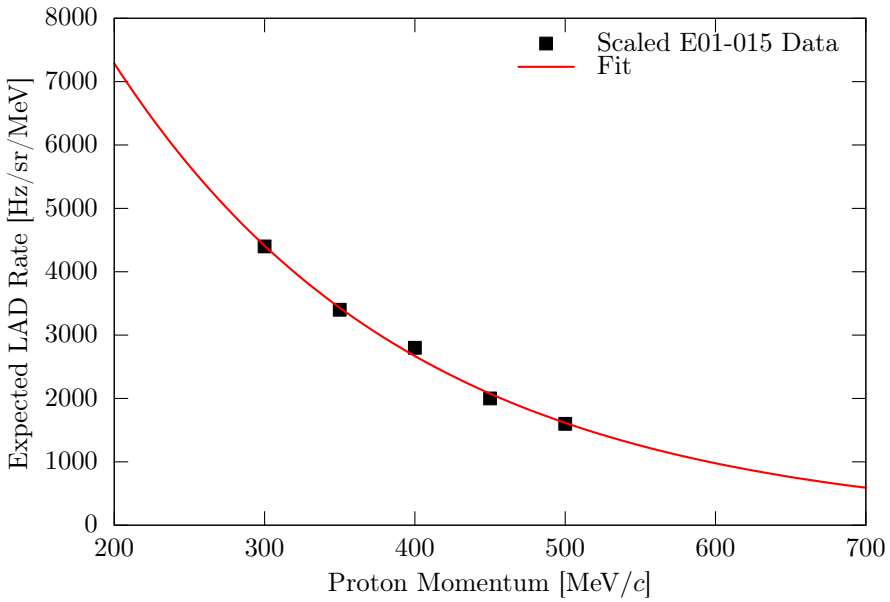

Figure 2: Fit to the proton singles rate measured by Big Bite at 90° in E01-015, but scaled to the proposal luminosity of 2×10^{36} cm^{-2}s^{-1} per nucleon

The data were fit with a two-parameter exponential function, i.e.,

$$f(x, a, b) = a \exp(-x/b), \tag{2}$$

with resulting parameters $a = 19,900$ Hz/sr/MeV and $b = 199$ MeV/c. These parameters result in a total rate of protons from 250–1000 MeV/c of 1.10 MHz/sr, slightly above the assumption of the proposal. Protons were generated down to 200 MeV/c, for which the total rate was 1.43 MHz/sr. Scaled to the new higher luminosity of 1.2×10^{37} cm^{-2}s^{-1} per nucleon (i.e., 6×10^{36} cm^{-2}s^{-1} per deuteron) results in rates of 6.60 MHz/sr and 8.58 MHz/sr respectively.

The total proton cross section over the proton generation range described in Table 1 (1.73 sr) is 2.48 μb.

The simulated background protons are offset in time by ±15 ns. This is small relative to the total proton time of flight (in the range of 25–125 ns) but adequately covers range of accepted protons due to the strict cuts that can be placed on the correlation of proton time-of-flight and energy deposition.

3 Simulation

After generation, the next task is to simulate the trajectories of the recoiling spectator protons, with the goal of accounting for multiple scattering in material. This is accomplished through the repository program `lad_sim`.

3.1 Multiple scattering

In this simulation, we assume that multiple scattering will change the direction of a particle's momentum vector, but not change its magnitude. As the particle crosses a thin plane of material, we randomly sample a re-scattering angle from a Gaussian distribution, with the width, σ_θ, given by:

$$\sigma_\theta = \frac{0.0136 \text{ GeV}}{\beta c p} \sqrt{\frac{2x}{X_0}} \left[1 + 1.038 \ln \frac{x}{X_0} \right], \tag{3}$$

where βc is the proton velocity, p is the proton momentum, and x/X_0 is the material thickness in units of radiation lengths. This approximation is suggested by the PDG, as eq. 27.10 [4]. The direction of the rescatter is assumed to be azimuthally symmetric.

3.2 Geometry

Table 2: Material included in the simulation

Object	Material	Thickness [μm]	Thickness [x/X_0]
Target liquid	Liquid deuterium	10,000	0.0013
Target wall	Aluminum	254	0.0029
Scattering Chamber Window	Aluminum	410	0.0046
GEMs	-	-	0.0030

The geometry of the scattering chamber, GEMs, and LAD were defined within the `lad_sim` program, for which a summary of the relevant parameters is given in Table 2.

Events begin in the liquid deuterium target cell, which is 20 cm long and 2 cm wide. The beam was assumed to be down the middle of the cell. The cell wall was 1/100" aluminum (i.e., 254 μm). The liquid deuterium in the cell and the cell wall were treated as a single re-scattering plane.

The scattering chamber was cylindrical, with a window positioned at a radius of 62.3 cm around the center of the target. The window was assumed to be 410 μm of aluminum, covering $\pm$7.5" above and below the height of the beam, and covering scattering angles of 90–157° relative to the beam direction. Only protons passing through the window were considered. All others were rejected at the simulation stage.

The two GEM detectors were positioned perpendicular to the 127° scattering angle, with positions of closest approach at 75 and 95 cm from the coordinate origin. The GEMs were assumed to be large enough to not limit the acceptance.

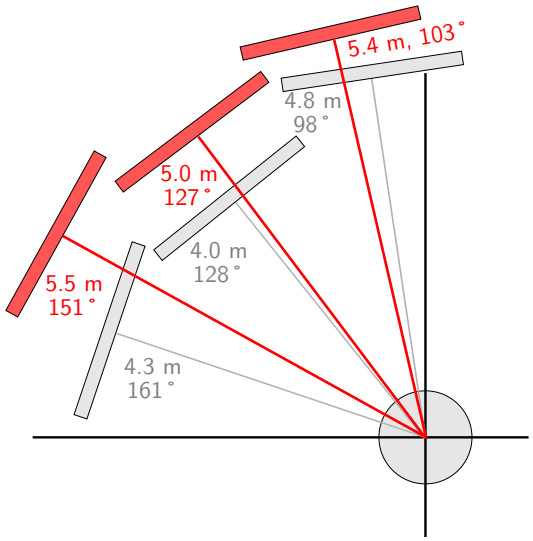

Figure 3: The placement of the LAD panels in this simulation (red), in comparison to the placement in the proposal (gray)

The three LAD planes were positioned perpendicular to the 103°, 127°, and 151° scattering angles, at center-line positions of 540 cm, 500 cm, and 550 cm respectively, shown in Fig. 3. All panels were assumed to be made of 11 panels with a width of 22 cm, and with a height of 4 m. The LAD panels were also assumed to limit the acceptance.

4 Digitization and Reconstruction

Both the LAD digitization, or detector response, and the event reconstruction were modeled by a program called `lad_digi`.

4.1 Digitization

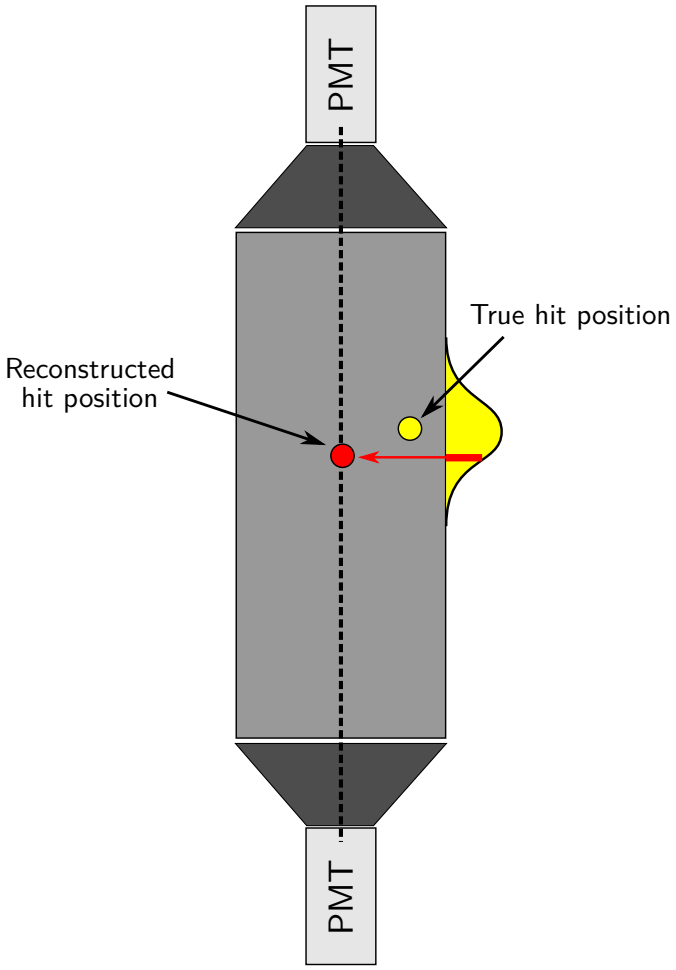

Figure 4: LAD hits were reconstructed along the central axis of the hit LAD bar, and were smeared in vertical position with a Gaussian random number according to the PMT resolution. The LAD bar here is not drawn to scale.

The GEMs were assumed to have a Gaussian hit position resolution, with a width of 100 μm in the local x direction (horizontal) and 100 μm in the local y direction (vertical). The local z direction (along the length of the track) was assumed to be perfectly known.

The response from LAD was modeled according to a 300 ps time resolution, independent of energy deposition. The speed of light within the plastic was assumed to be 15 cm/ns, i.e., the assumed index of refraction was assumed to be $n = 2$. Hits in LAD were reconstructed at the position of the mid-line of the hit scintillator paddle (illustrated in Fig. 4. Since the vertical hit position will be reconstructed from the time difference between the signals in the top and bottom PMTs, the vertical hit position was smeared according to:

$$\sigma_y = \frac{c}{n\sqrt{2}}\sigma_{\mathrm{PMT}} \approx 3.2 \text{ cm}$$

Similarly, the hit time resolution was assumed to be

$$\sigma_t = \sqrt{2}\sigma_{\mathrm{PMT}} \approx 424 \text{ ps}$$

LAD was assumed to be able to reconstruct the momentum of protons from dE/dx with a Gaussian resolution of 20 MeV/c.

In order to compare the proton vertex (as reconstructed by the GEMs) with the electron vertex reconstructed by either the HMS or SHMS, a resolution model for the spectrometers was needed. Based on preliminary Hall C analyses, we assumed a Gaussian `ytar` resolution of 1 mm, corresponding to a vertex resolution of 1 mm/$\sin\theta$.

4.2 Reconstruction

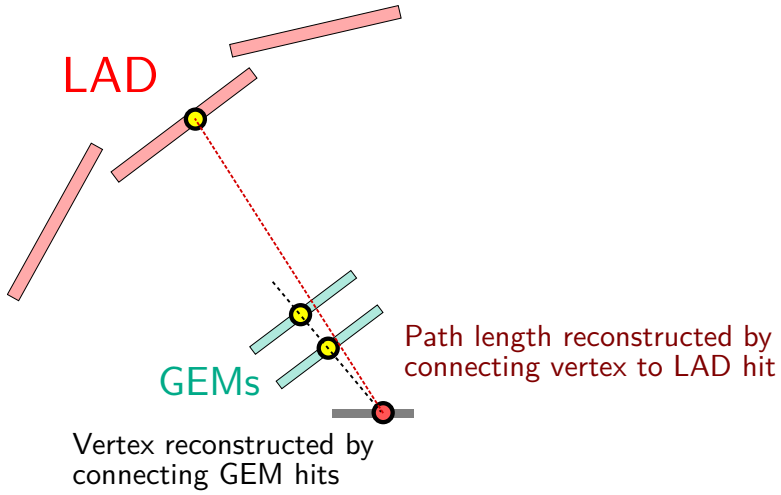

Figure 5: The proton vertex was first determined by connecting a straight line between reconstructed GEM hits, ignoring the LAD hit. The proton path length (needed to determine momentum from time-of-flight) was reconstructed as the straight-line distance between the reconstructed proton vertex and the reconstructed LAD hit. This diagram is highly not to scale.

For these simulations, a simplistic event reconstruction model was employed. The proton vertex position was determined by connecting the two reconstructed GEM hits. The proton momentum was determined from the reconstructed hit time in LAD, and the reconstructed path length, found by connecting the proton vertex position with the position of the LAD hit, illustrated in Fig. 5.

5 Analysis

The event selection was performed by a program called `lad_analysis`. Cuts on vertex correlation and proton energy deposition in LAD were performed to reject background. Further cuts were applied to select good events in DIS kinematics.

5.1 Vertex Cut

The vertex correlation resolution depends on both the electron scattering angle θ_e and the recoil proton angle θ_r, with characteristic $1/\sin\theta$ dependence (illustrated in Fig. 6). To account for this, a we employed a variable vertex correlation cut:

$$|z_e^{\mathrm{rec.}} - z_r^{\mathrm{rec.}}| < N_\sigma \times \sqrt{(\sigma_r/\sin\theta_r)^2 + (\sigma_e/\sin\theta_e)^2}. \quad (4)$$

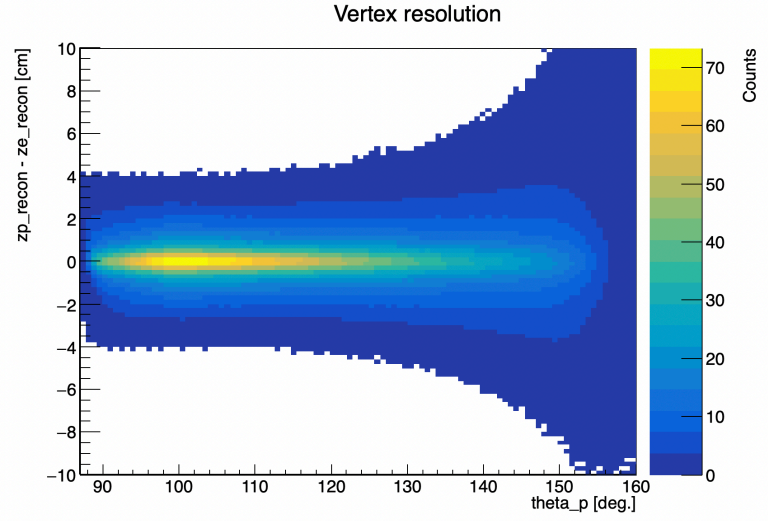

Figure 6: The difference between reconstructed proton and electron vertex positions as a function of proton angle. The vertex resolution degrades for the most backward protons.

where N_σ, the number of σ accepted by the cut was set to 2. The electron resolution σ_e was taken to be the assumed `ytar` resolution of the spectrometers, i.e., 1 mm. The recoil proton resolution factor, σ_r, was determined by a fit to the distribution of the difference in reconstructed and true proton vertices, for proton near 90°. The exact value of σ_r is slightly different for the two spectrometers, but for both it was approximately 1 cm.

5.2 Energy Deposition

Recoil protons were required to have a momentum reconstructed from energy deposition within 40.4 MeV/c of that reconstructed from time-of-flight, corresponding to an approximately 2σ cut.

5.3 Event Selection Criteria

Good DIS events were required to have

- $Q^2 > 2$ GeV$^2/c^2$
- $W' > 2$ GeV^2
- $\theta_{qr} > 110°$
- $p_r > 275$ MeV/c

where θ_{qr} is the angle between the momentum transfer vector $\vec{q}$ and the recoil proton momentum vector $\vec{p}_r$. These cuts were all made based on reconstructed quantities.

Events were also required to have the electron ϕ within the azimuthal acceptance of the spectrometers. This acceptance was estimated from nominal values of the spectrometer solid angle (Ω) and `yptar` coverage ($\Delta y'_{\rm tar}$), i.e.,

$$\Delta\phi = \pm\frac{\Omega}{2\Delta y'_{\rm tar}\sin\theta_e}$$

The values assumed for the two spectrometers are shown in Table 3.

The kinematic coverage of events passing all selection cuts are shown in Fig. 7 and 8.

Table 3: Spectrometer Acceptance Parameters

Spectrometer	Ω [msr]	$\Delta y'_{\text{tar}}$ [mrad]	Side
HMS	6.72	28	Beam Right
SHMS	3.84	24	Beam Left

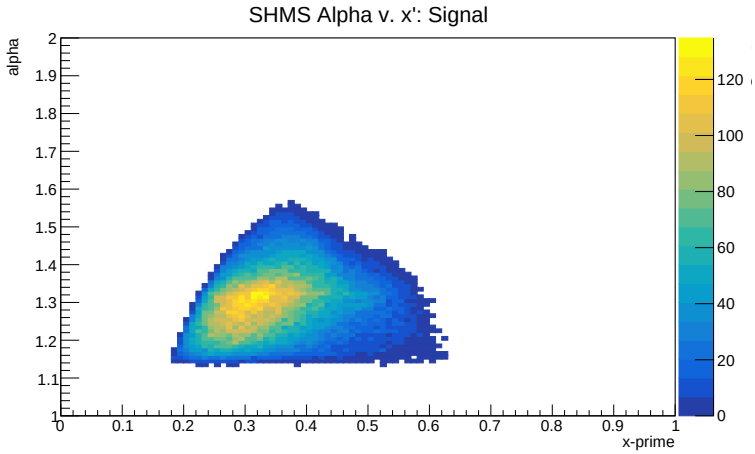

Figure 7: Here we see the accepted α_s versus x' from SHMS signal data with the high x' threshold 0.5. The same for background data can be found in the Appendix C Figure 13.

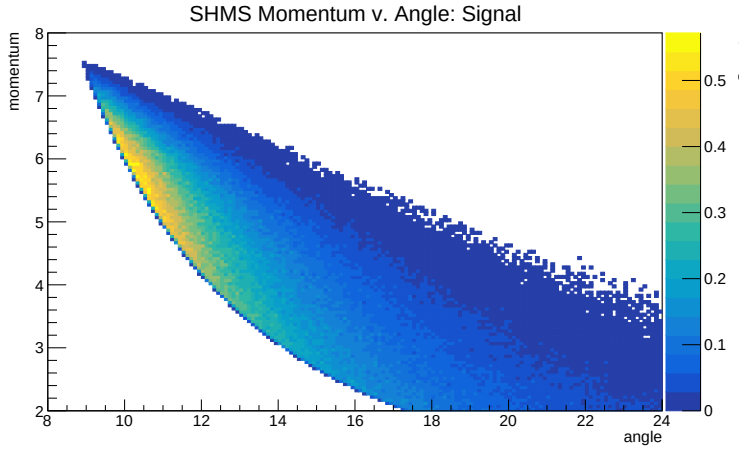

Figure 8: Here we see the accepted electron angle versus momentum from SHMS signal data with high x' threshold 0.5. The same for background data can be found in Appendix C Figure 14.

6 Optimization

To determine the settings which minimize the statistical error, we wrote five optimization programs. The settings we consider for optimization are the time distribution that the spectrometers spend in the high x' and low x' settings, the angle of the high and low x' settings, and the common central momentum value of both settings. These programs, which are found in `lad_sim/optimization`, require as input both signal and background files for both the SHMS and HMS spectrometers. The programs return both the optimized settings and a series of arrays (in numpy syntax) containing statistical error and the signal and background counts at low x' ($0.25 < x' < 0.35$) and for x' greater than some threshold value. The total integral of low x' and high x' events come from both settings, i.e., low x' events are collected in both the low x' and high x' settings and vice versa. As a baseline, we compared against the values listed in the original LAD proposal, i.e., 300 hours for each spectrometer at the low-x' setting (13.5°, 4.4 GeV/c) and 520 hours at the high-x' setting (17.0°, 4.4 GeV/c).

The five programs are:

- `optimization/default`: uses the proposal settings without optimization
- `optimization/opt1`: minimizes the statistical error with respect to the time distribution in each setting.
- `optimization/opt2`: minimizes error with respect to time distribution and the high x' angular position.
- `optimization/opt3` adds a third tier to this optimization, further minimizing with respect to low x' angular position.
- `optimization/opt4` minimizes error with respect to all settings previously mentioned, and with respect to the common momentum setting.

Optimization is performed with respect to the relative statistical uncertainty on the ratio:

$$R(\alpha) \equiv \frac{N_{\text{sig.}}^{\text{high } x'}(\alpha)}{N_{\text{sig.}}^{\text{low } x'}(\alpha)}, \tag{5}$$

where $N_{\text{sig.}}^{\text{high } x'}(\alpha)$ is the number of high-x' signal counts, and $N_{\text{sig.}}^{\text{low } x'}(\alpha)$ is the number of low-x' signal counts for a given α bin. The uncertainty is given by:

$$\frac{\delta R}{R} = \sqrt{\left(\frac{\delta N_{\text{sig.}}^{\text{high } x'}}{N_{\text{sig.}}^{\text{high } x'}}\right)^2 + \left(\frac{\delta N_{\text{sig.}}^{\text{low } x'}}{N_{\text{sig.}}^{\text{low } x'}}\right)^2}, \tag{6}$$

where the α dependence is implicit.

The number of signal counts must be extracted from the number of total counts, N, in a bin, minus the number of background counts, $N_{\text{bkg.}}$. Thus, $\delta N_{\text{sig.}} = \sqrt{N} = \sqrt{N_{\text{sig.}} + N_{\text{bkg.}}}$, and we have

$$\frac{\delta R}{R} = \sqrt{\frac{N_{\text{sig.}}^{\text{high } x'} + N_{\text{bkg.}}^{\text{high } x'}}{(N_{\text{sig.}}^{\text{high } x'})^2} + \frac{N_{\text{sig.}}^{\text{low } x'} + N_{\text{bkg.}}^{\text{low } x'}}{(N_{\text{sig.}}^{\text{low } x'})^2}}. \tag{7}$$

The optimum was chosen to have the smallest sum of squared errors for six α bins, centered at 1.175, 1.225, 1.275, 1.325, 1.375, and 1.425, i.e.,

$$\text{Tot. Squared Error} \equiv \sum_{\alpha=1.175}^{1.425} \left(\frac{\delta R}{R}\right)^2. \tag{8}$$

Note that the proposal also included projections for a 1.475 bin, which we no longer consider.

The proposal used a high-x' threshold of $x' > 0.45$. With the additional background rejection afforded by the GEMs, we decided to additionally consider optimization for threshold of $x' > 0.5$. We consider the two threshold cases separately.

Table 4: Optimization Results, High x' Threshold of 0.45

Case	Time Dist.	High x' θ	Low x' θ	Mom. [GeV/c]	Tot. Squared Error
Proposal	300/520 hrs	17°	13.5°	4.4	0.0042
1	300/520 hrs	17°	13.5°	4.4	0.0131
2	**200/620 hrs**	17°	13.5°	4.4	0.0127
3	**160/660 hrs**	**16.1**°	13.5°	4.4	0.0105
4	**120/700 hrs**	**16.1**°	**12.4**°	4.4	0.0103
5	**120/700 hrs**	**16.1**°	**12.4**°	**4.45**	0.0100

7 Results

Tables 4 and 5 show the results of our optimizations for several different cases in which different parameters were allowed to vary. In each line of the table, emboldened quantities were allowed to vary, while all others were held fixed.

When keeping the same $x' > 0.45$ threshold from the proposal, we found that the settings were already well optimized. Our simulation prefers a slight decrease in angles, and a slight adjustment of the time spent in the two settings, but the reduction in total error from these changes is modest.

When optimizing with respect to an $x' > 0.5$ threshold, we found two changes that can significantly improve the total squared error. First, we find that spending significantly more time in the high x' setting is highly beneficial. Second, we found a significant improvement by reducing the common momentum setting of the spectrometers from 4.4 GeV/c to 3.8 GeV/c.

The details of each optimization case are described in the subsequent sections.

7.1 Optimizing with an $x' > 0.45$ Threshold

Fig. 9 shows the projected statistical uncertainties when optimizing with respect to a high-x' threshold of 0.45, in comparison to the projected uncertainty of the proposal, which had a significantly different geometry, lower luminosity, and no GEMs. The results are further discussed below.

7.1.1 Case 1: Default Proposal Settings

For this case, we use the default settings from the LAD Proposal: Time distributed 320/500 hours between low and high x' settings respectively; High x' central angle at 17°; Low x' central angle at 13.5°; Common momentum setting at 4.4 GeV/c. This case uses the program `optimization/default` applied to background and signal analysis files for high x' threshold 0.45.

7.1.2 Case 2: Adjusting Hours

For Case 2, we minimize the statistical uncertainty with respect to the time distribution between low and high x' angular positions, and use the default spectrometer settings: High x' central angle at 17°; Low x' central angle at 13.5°; Common momentum setting at 4.4 GeV/c. This case uses the program `optimization/opt1` applied to background and signal analysis files for high x' threshold 0.45. We find that a slight decrease in uncertainty can come from using 200/620 hours, rather than the default 300/520 hours listed in the proposal. The statistical uncertainty is still larger than the proposal by approximately a factor of two.

7.1.3 Case 3: Adjusting Hours, High x' angle

For this case, we optimize with respect to the time distribution and the high x' central angle, while keep the low x' central angle at 13.5° and the common momentum setting at 4.4 GeV/c. We find slight improvement by adjusting the central angle forward to 16.1°, and using 160 hours in the low x' setting.

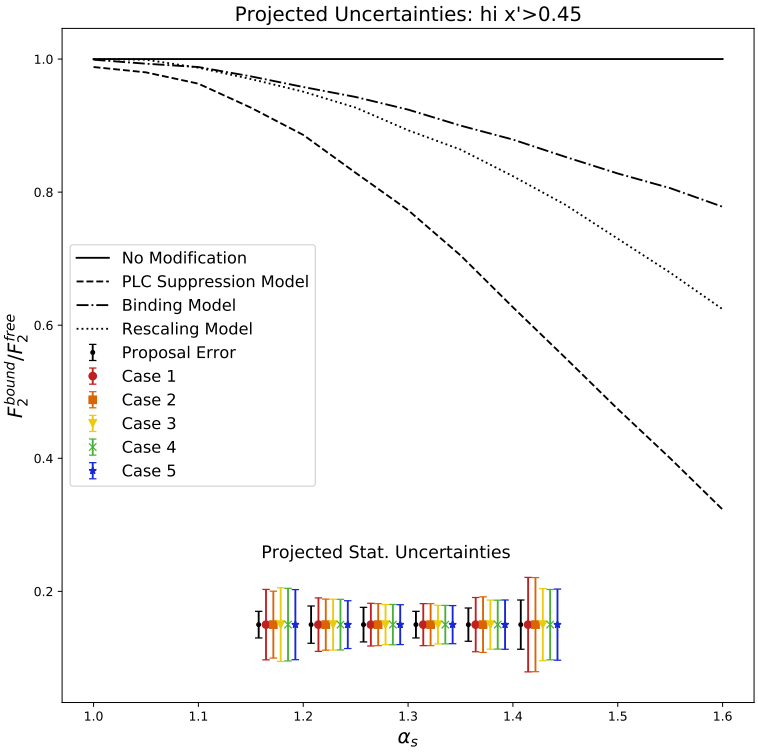

Figure 9: The statistical uncertainty of the structure function ratio for cases with a high x' threshold of 0.45, compared to theoretical expectations from Ref. [5]

7.1.4 Case 4: Adjusting Hours, High and Low x' angles

For our fourth case, we maintain the 4.4 GeV/c common momentum setting as originally proposed, but we adjust the time distribution and both central angles (for high and low x' settings) to minimize statistical error. We find this optimization yields central angles 16.1° for high x' and 12.4° for low x', and 120/700 hours in the low/high x' settings, but that these changes only marginally decrease the total squared error.

7.1.5 Case 5: Adjusting Hours, High and Low x' angles, Momentum Setting

In this final optimization, we adjust the time distribution, central angles for low and high x' settings, and the common momentum setting. We find the optimized settings to be 120/700 hours in the low/high x' settings, 16.1° as the high x' central angle, 12.4° as the low x' central angle, and common momentum setting 4.45 GeV/c.

7.2 Optimizing with an $x' > 0.5$ Threshold

Table 5: Optimization Results, High x' Threshold of 0.5

Case	Time Dist.	High x' θ	Low x' θ	Mom. [GeV/c]	Tot. Squared Error
1	300/520 hrs	17°	13.5°	4.4	0.0855
2	**60/760 hrs**	17°	13.5°	4.4	0.0574
3	**50/770 hrs**	**16.3°**	13.5°	4.4	0.0531
4	**50/770 hrs**	**16.3°**	**12.2°**	4.4	0.0509
5	**50/770 hrs**	**17.4°**	**13.4°**	**3.8**	0.0274

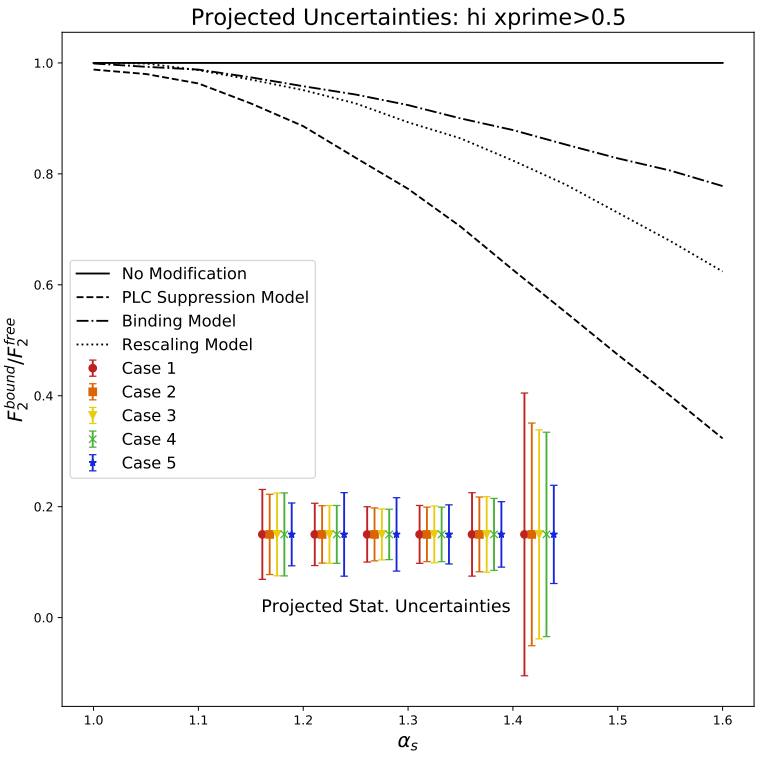

Figure 10: The statistical uncertainty of the structure function ratio for cases with a high x' threshold of 0.5, compared to theoretical expectations from Ref. [5]

Fig. 10 shows the projected statistical uncertainties when optimizing with respect to a high-x' threshold of 0.5. The results are further discussed below.

7.2.1 Case 1: Default Proposal Settings, High threshold $x' > 0.5$

We use the default settings as listed for Case 1, but with a higher x' threshold, which should yield a more impactful result. We use the settings: Time distributed 320/500 hours between low and high x' angular positions (respectively); High x' central angle at 17°; Low x' central angle at 13.5°; Common momentum setting at 4.4 GeV/c. We find that the total squared error is a factor of six worse than when using an $x' > 0.45$ threshold.

7.2.2 Case 2: Adjusting Hours, High threshold $x' > 0.5$

We first optimized with respect to the time distribution, while using the default spectrometer settings. We find that the total statistical uncertainty can be reduced by rebalancing the time to only a mere 60 hours in the low x' setting, and using the rest of the time to measure in the slower-counting high-x' setting. This is quite an extreme departure from the proposal run plan.

7.2.3 Case 3: Adjusting Hours, High x' angle, High threshold $x' > 0.5$

For this case, we optimize with respect to time distribution and the high x' central angle, while keeping the low x' central angle at 13.5° with the common momentum setting 4.4 GeV/c as in the proposal. We find marginal improvement by moving the central angle forward to 16.3°, and using only 50 hours to measure in the low x' setting.

7.2.4 Case 4: Adjusting Hours, High and Low x' angles, High threshold $x' > 0.5$

For this case, we minimize our uncertainty with respect to time distribution, and both high and low x' central angles. We still use the common momentum setting 4.4 GeV/c. We find marginal improvement by using 12.2° and 16.3° for the low x' and high x' settings respectively, and with 50 hours spent in the lo x' position.

7.2.5 Case 5: Adjusting Hours, High and Low x' angles, Momentum Setting, High threshold $x' > 0.5$

For our final optimization, we optimize with respect to time distribution, high and low x' central angles, and the common momentum setting. We find a factor of two improvement by using a 3.8 GeV/c momentum setting, with central angles of 13.4° and 17.4°, with 50 hours spent in the low x' position.

8 Conclusions

We have used an updated LAD simulation to reevaluate the expected statistical uncertainty that LAD can achieve given the new detector placement, new luminosity, and potentially new high-x' threshold. We estimate the uncertainty to be larger than that predicted in the proposal even with the use of GEMs for background suppression and at the higher luminosity of 6×10^{36} cm^{-2}s^{-1} per deuteron. The limiting factor continues to be the random coincidence background. We find that, when using a high-x' threshold of $x' > 0.45$, as in the proposal, the proposal settings are already well-optimized. However, when using an x' threshold of $x' > 0.45$, we see two ways to significantly improve the statistical error:

1. spending as much running time as possible in the high-x' setting,
2. reducing the central momentum of the spectrometers.

The first recommendation can be considered even during data taking, after considering the actual rates of signal and background. The second recommendation may cause problems because of the proposed calibration using elastic scattering on hydrogen. This may require the spectrometers to sit at too far back an angle to catch elastics. This recommendation must be considered within the context of the calibration plan.

Further optimizations should be undertaken with the goal of improving accuracy. There are several areas where the accuracy of this study can be improved. In order of importance.

- The inclusive electron generator used in this study has already been shown to do a poor job at reproducing CLAS12 Run Group B (RG-B) data on deuterium. We should consider using a parameterization of F_2^d, bench-marking the normalization against RG-B data, and replacing the generator used in this study. What is particularly alarming is that the normalization of this generator sets the background rate, which in turn is the limiting factor for the statistical precision.
- The background rate in the GEMs must be modeled in detail. It remains to be seen what kind of background rate they will be subject to, and how many low-energy photon hits will occur per unit area, but this background will be the primary concern for analyzing data from the GEMs and the eventual suppression of random background.
- This study could improve in the detail in which the detectors are modeled. So far, we take no account of the spectrometer optics. Improvements should make use of the SHMS and HMS implementations in the SIMC package. The target, scattering chamber, GEMs and LAD detector ought to be properly modeled in Geant4.

These concerns largely affect the statistical uncertainty that can be achieved by changing the background rate. They probably have minimal impact on the optimal spectrometer settings. Therefore, while the eventual error bars may change, we have confidence in the angle and momentum settings recommended here.

References

[1] O. Hen *et al.*, "In medium nucleon structure functions, src, and the emc effect." Proposal to Jefferson Lab PAC 38, 2011.

[2] W. Cosyn and M. Sargsian, "Final-state interactions in semi-inclusive deep inelastic scattering off the Deuteron," *Phys. Rev. C*, vol. 84, p. 014601, 2011.

[3] A. Schmidt, "BAND experiment: physics motivation." Talk presented at the CLAS RG-B Experiment Readiness Review, February 2018.

[4] M. Tanabashi *et al.*, "Review of particle physics," *Phys. Rev. D*, vol. 98, p. 030001, 8 2018.

[5] W. Melnitchouk, M. Sargsian, and M. Strikman, "Probing the origin of the EMC effect via tagged structure functions of the deuteron," *Z. Phys. A*, vol. 359, pp. 99–109, 1997.

A Background to Signal Ratios

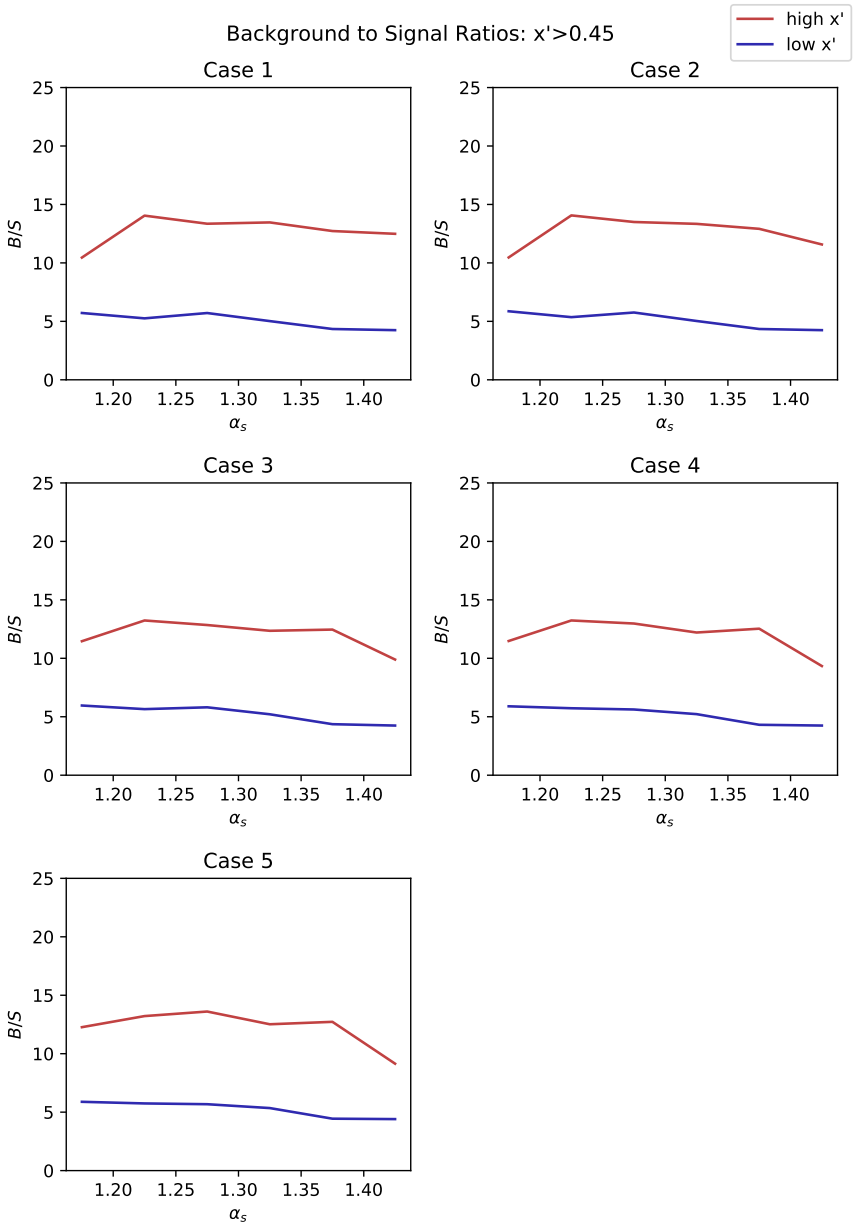

Figure 11: The background to signal ratios for all cases for the high x' threshold of 0.45

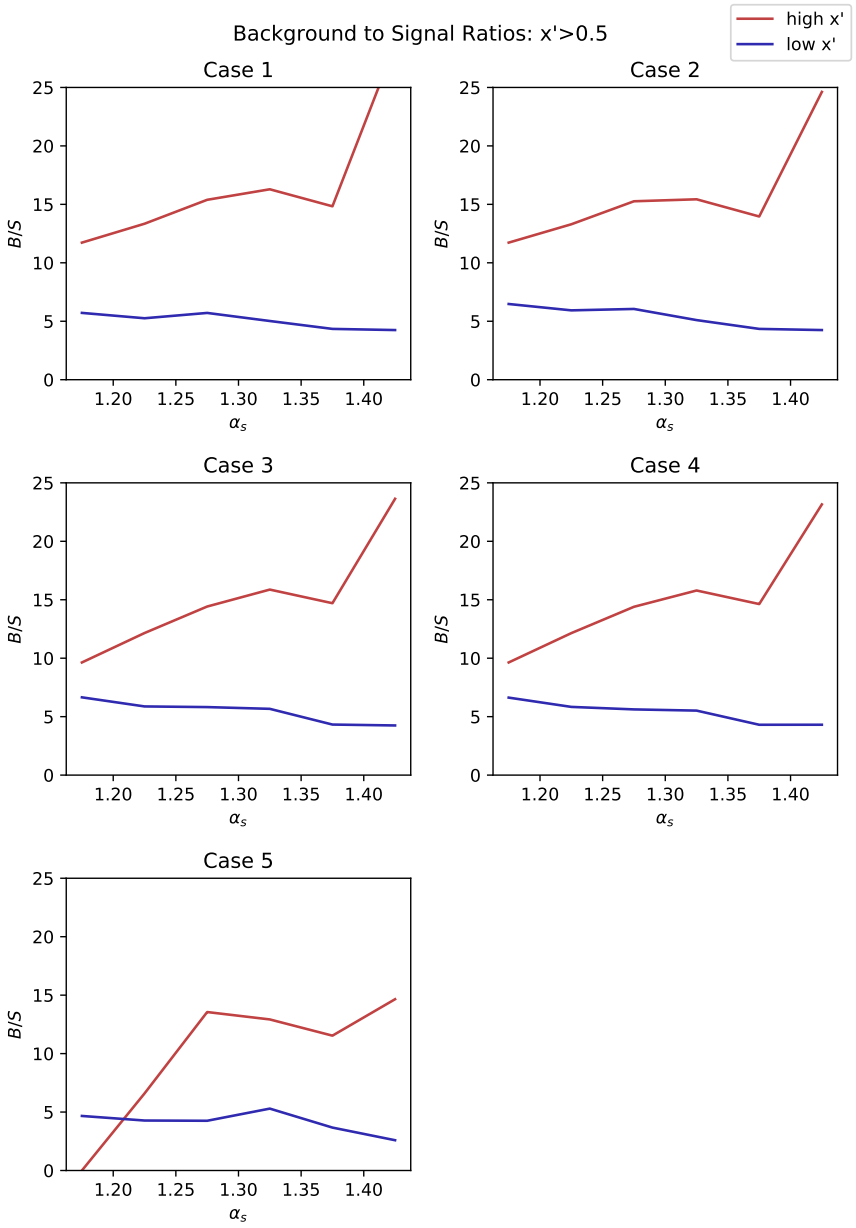

Figure 12: The background to signal ratios for all cases for the high x' threshold of 0.5

B Background and Signal Event Counts

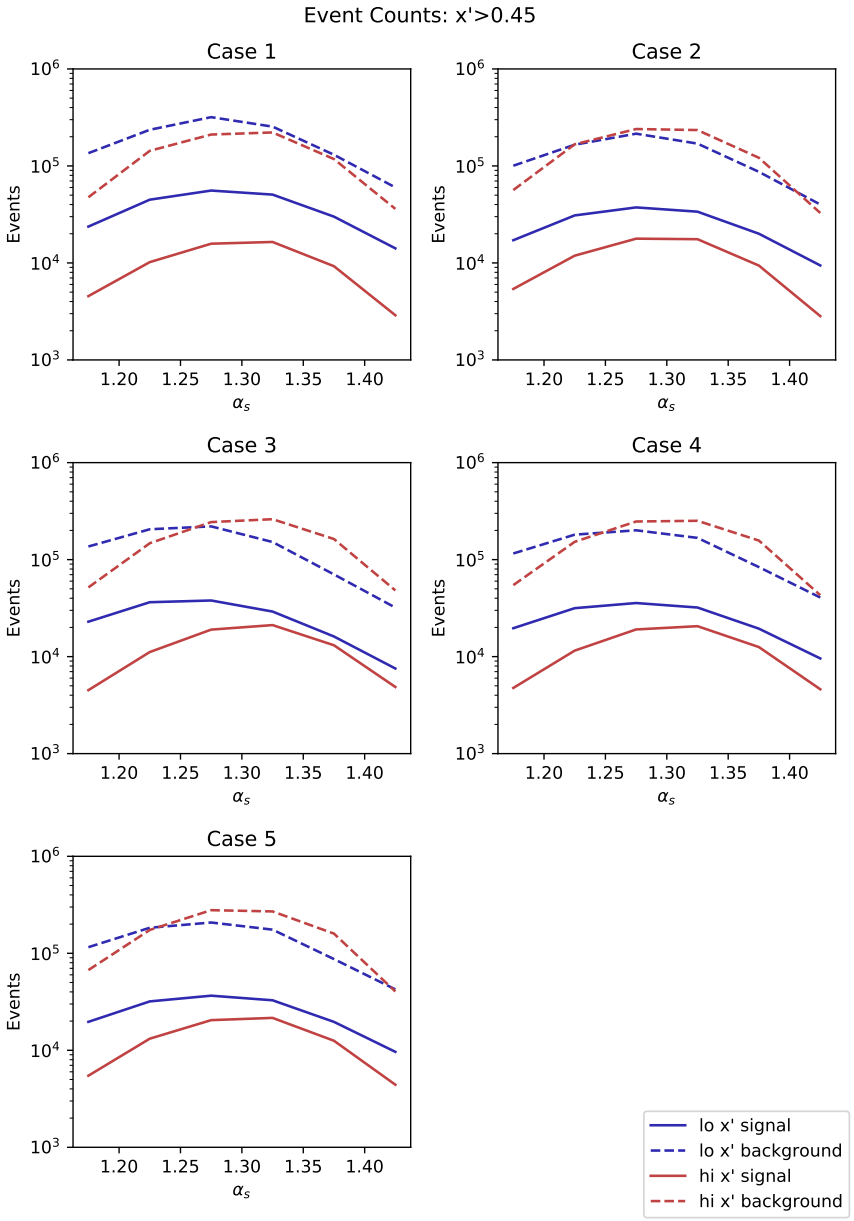

Figure 13: The event counts for all cases for the high x' threshold of 0.45

Table 6: Counts, High x' Threshold of 0.45

Opt. Case	α_s Bin	Low x' Signal	High x' Signal	Low x' Bkg.	High x' Bkg.
Case 1	1.15–1.20	23698	4548	135441	47553
	1.20–1.25	44895	10196	235978	143193
	1.25–1.30	55746	15788	318418	210785
	1.30–1.35	50650	16451	254342	221479
	1.35–1.40	30011	9252	130415	117742
	1.40-1.45	14138	2888	60040	36072
Case 2	1.15–1.20	17150	5394	100549	56456
	1.20–1.25	30892	11882	165556	167101
	1.25–1.30	37367	17794	215086	240192
	1.30–1.35	33770	17570	169903	234373
	1.35–1.40	20007	9396	86944	121343
	1.40-1.45	9425	2829	40027	32754
Case 3	1.15–1.20	22910	4512	136565	51711
	1.20–1.25	36379	11150	205601	147577
	1.25–1.30	37902	18984	220122	243873
	1.30–1.35	29147	21138	151898	261102
	1.35–1.40	16126	13094	70379	163112
	1.40-1.45	7540	4866	32021	48142
Case 4	1.15–1.20	19630	4755	115709	54585
	1.20–1.25	31585	11530	180896	152616
	1.25–1.30	35685	19054	200595	247230
	1.30–1.35	32072	20599	167553	251411
	1.35–1.40	19420	12547	83743	157258
	1.40-1.45	9576	4607	40668	43016
Case 5	1.15–1.20	19648	5473	115628	67144
	1.20–1.25	31927	13178	183433	174184
	1.25–1.30	36572	20461	207703	278423
	1.30–1.35	32789	21587	175388	270219
	1.35–1.40	19638	12545	87209	159639
	1.40-1.45	9640	4419	42466	40420

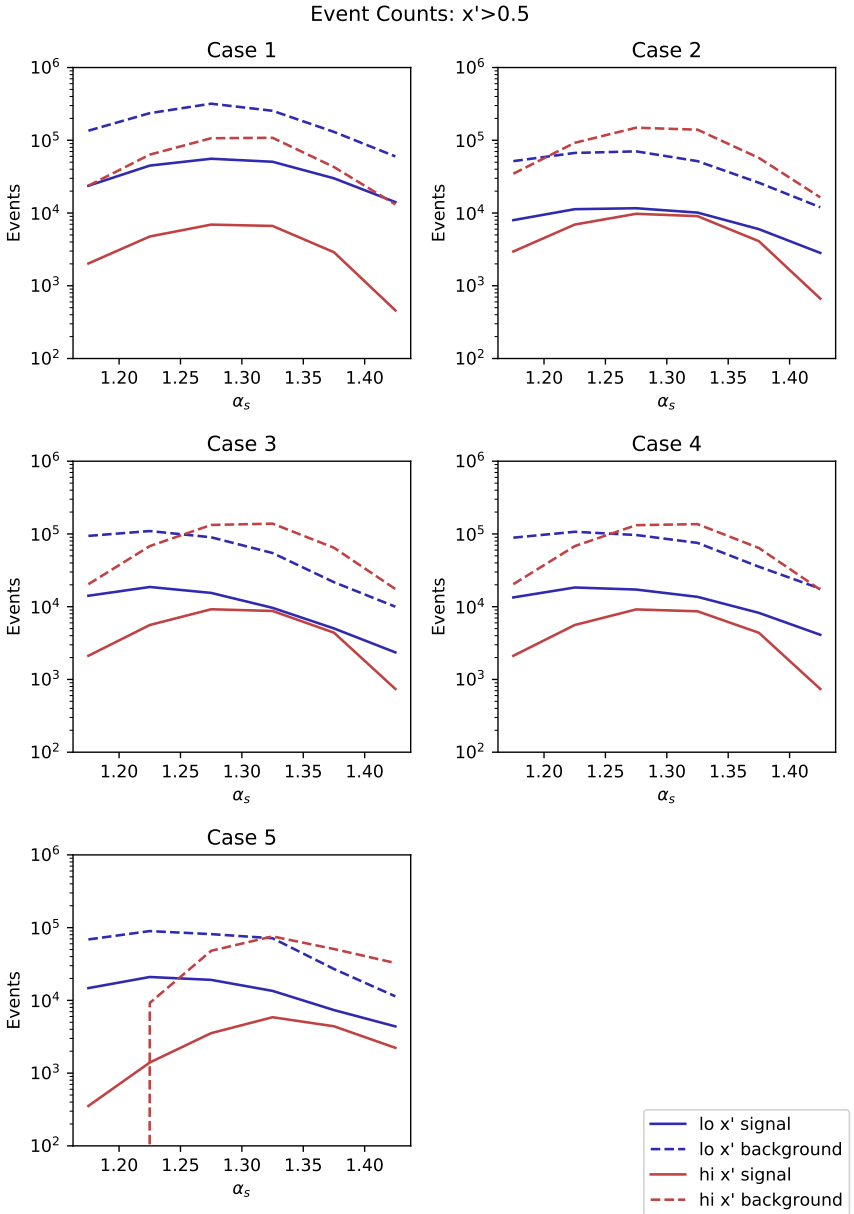

Figure 14: The event counts for all cases for the high x' threshold of 0.5

Table 7: Counts, High x' Threshold of 0.5

Opt. Case	α_s Bin	Low x' Signal	High x' Signal	Low x' Bkg.	High x' Bkg.
	1.15–1.20	23698	2025	135441	23742
	1.20–1.25	44895	4760	235978	63508
Case 1	1.25–1.30	55746	6931	318418	106658
	1.30–1.35	50650	6645	254342	108241
	1.35–1.40	30011	2893	130415	42906
	1.40-1.45	14138	459	60040	13140
	1.15–1.20	7983	2959	51701	34701
	1.20–1.25	11288	6937	66964	92238
Case 2	1.25–1.30	11636	9757	70421	148918
	1.30–1.35	10137	9061	51687	139836
	1.35–1.40	6002	4099	26083	57228
	1.40-1.45	2828	667	12008	16410
	1.15–1.20	14145	2115	94100	20382
	1.20–1.25	18668	5602	109655	68089
Case 3	1.25–1.30	15473	9223	90019	133000
	1.30–1.35	9649	8735	54695	138630
	1.35–1.40	5027	4399	21736	64692
	1.40-1.45	2356	741	10007	17507
	1.15–1.20	13415	2115	88913	20382
	1.20–1.25	18363	5600	107134	68012
Case 4	1.25–1.30	17215	9174	96743	132079
	1.30–1.35	13662	8649	75372	136587
	1.35–1.40	8231	4382	35444	64121
	1.40-1.45	4111	740	17712	17138
	1.15–1.20	14756	354	68857	0.0
	1.20–1.25	20969	1400	89640	9230
Case 5	1.25–1.30	19140	3546	81427	48071
	1.30–1.35	13506	5869	71506	75840
	1.35–1.40	7361	4405	27023	50814
	1.40-1.45	4390	2228	11372	32648

C Background Distributions

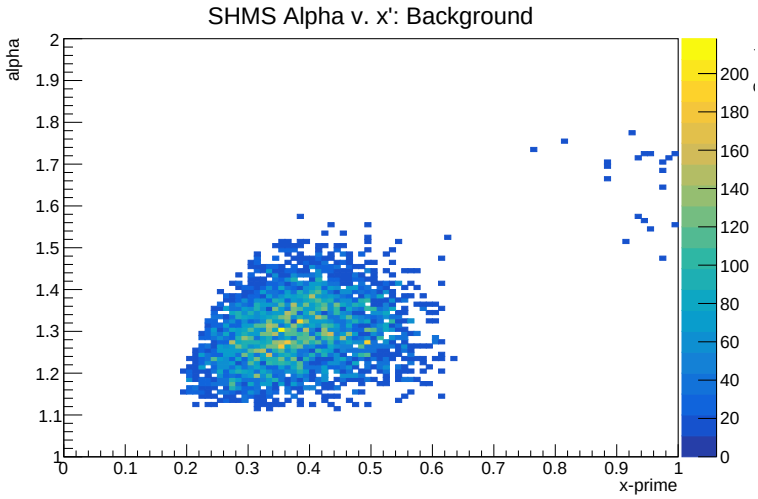

Figure 15: Here we see the accepted α_s versus x' from SHMS background data with high x' threshold of 0.5.

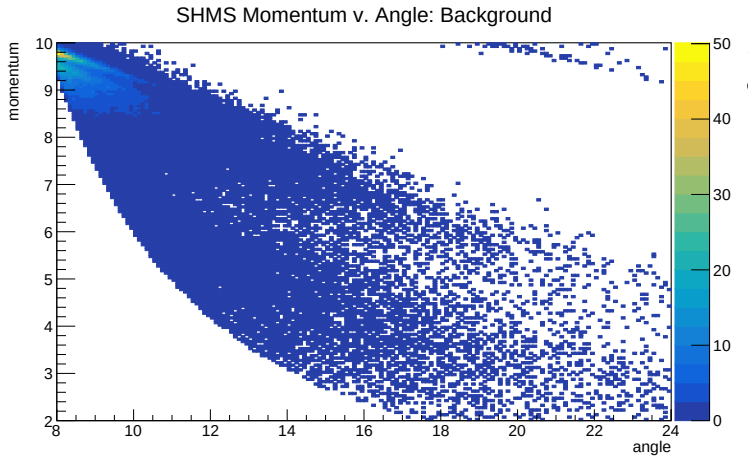

Figure 16: Here we see the accepted electron angle versus momentum from SHMS background data with high x' threshold of 0.5.